Cerebral Cortex, 2016, 1–11

doi: 10.1093/cercor/bhw130
Original Article

ORIGINAL ARTICLE

Remodeling of Dendritic Spines in the Avian Vocal Motor Cortex Following Deafening Depends on the Basal Ganglia Circuit

Xin Zhou[1], Xin Fu[1], Chun Lin[4], Xiaojuan Zhou[1], Jin Liu[1], Li Wang[3], Xinwen Zhang[4], Mingxue Zuo[1], Xiaolong Fan[1], Dapeng Li[2] and Yingyu Sun[1]

[1]Beijing Key Laboratory of Gene Resource and Molecular Development, Laboratory of Neuroscience and Brain Development, College of Life Sciences, Beijing Normal University, Beijing 100875, China, [2]State Key Laboratory of Brain and Cognitive Sciences, [3]Center for Biological Imaging (CBI), Institute of Biophysics, Chinese Academy of Science, Beijing 100101, China and [4]Department of Biology, Hainan Normal University, Haikou 571158, China

Address correspondence to Yingyu Sun, Email: sunyingyu@bnu.edu.cn; Dapeng Li, Email: lidapengibp@hotmail.com

Abstract

Deafening elicits a deterioration of learned vocalization, in both humans and songbirds. In songbirds, learned vocal plasticity has been shown to depend on the basal ganglia-cortical circuit, but the underlying cellular basis remains to be clarified. Using confocal imaging and electron microscopy, we examined the effect of deafening on dendritic spines in avian vocal motor cortex, the robust nucleus of the arcopallium (RA), and investigated the role of the basal ganglia circuit in motor cortex plasticity. We found rapid structural changes to RA dendritic spines in response to hearing loss, accompanied by learned song degradation. In particular, the morphological characters of RA spine synaptic contacts between 2 major pathways were altered differently. However, experimental disruption of the basal ganglia circuit, through lesions in song-specialized basal ganglia nucleus Area X, largely prevented both the observed changes to RA dendritic spines and the song deterioration after hearing loss. Our results provide cellular evidence to highlight a key role of the basal ganglia circuit in the motor cortical plasticity that underlies learned vocal plasticity.

Key words: basal ganglia, dendritic spine, songbird, vocal motor cortex, vocal plasticity

Introduction

Learned vocalization is a rare trait that is shared by humans and songbirds, but not found in most mammals (Jarvis 2004). In most vocal learning species, some level of vocal plasticity is maintained throughout life. For example, adults who are deafened after they learn to speak (post-lingually) suffer a gradual deterioration in speech production (Waldstein 1990; Lane and Webster 1991; Cowie and Douglas-Cowie 1992). Likewise, in zebra finches and Bengalese finches, the most studied songbird species, the stereotyped adult songs "decrystallize", becoming less stereotyped, following deafening or distorted feedback (Nordeen and Nordeen 1992; Okanoya and Yamaguchi 1997; Woolley and Rubel 1997; Leonardo and Konishi 1999; Lombardino and Nottebohm 2000; Horita et al. 2008; Tschida and Mooney 2012). However, the neural substrate underlying adult vocal plasticity is still poorly defined. Understanding the biological basis of plasticity mechanisms in the vocal system is especially important for insights into speech deficits and rehabilitation after acquired brain damage or post-lingual deafness (Bashir et al. 2010; Pasley and Knight 2013; Lazard et al. 2014).

Birdsong has been a tractable model system for investigating the neural basis of learned vocal control and plasticity (Doupe et al. 2005; Brainard and Doupe 2013), largely due to its

underlying specialized and well-delineated neural circuitry, known as the song system (Nottebohm et al. 1976; Bottjer et al. 1984). This consists of 2 interconnected pathways, the descending vocal motor pathway (VMP) and the anterior forebrain pathway (AFP). In the VMP, the premotor nucleus HVC (proper name) projects to the robust nucleus of the arcopallium (RA), a motor cortex analog, which shares molecular similarities with human laryngeal motor cortex and connects directly to brainstem motor neurons for vocal production (Pfenning et al. 2014; Simonyan 2014). The AFP, homologous to the mammalian basal ganglia-thalamo-cortical circuits, connects HVC and RA indirectly via the basal ganglia homolog, Area X, the anterior portion of the dorsal lateral nucleus of the medial thalamus (aDLM, Horita et al. 2012), and the lateral part of the magnocellular nucleus of the nidopallium (LMAN).

Intensive studies in humans and mammals indicate that the basal ganglia circuit contributes to motor control and is involved in numerous movement disorders (Albin et al. 1989; Graybiel et al. 1994), including speech deficits (Simonyan et al. 2012), perhaps by influencing motor cortex activity and plasticity (Ashby et al. 2010; Kishore et al. 2014). By lesioning or inactivating the LMAN, or lesioning Area X, it has been demonstrated that the AFP is essential for adult vocal plasticity (Williams and Mehta 1999; Brainard and Doupe 2000; Kao et al. 2005; Thompson et al. 2007; Andalman and Fee 2009; Warren et al. 2011; Kojima et al. 2013). However, the underlying mechanisms are yet unclear. Previous studies indicate that the AFP could play a direct role in initial changes in song behavior, induced either by reinforcement training or deafening, whereas enduring changes may be encoded in the VMP (Andalman and Fee 2009; Nordeen and Nordeen 2010), within which the motor cortex RA is a promising site for such plasticity. Several studies have shown a close correlation between RA plasticity and vocal changes. For example, remarkable structural and functional synaptic changes are found in the RA during the period of vocal learning (Herrmann and Arnold 1991; Mooney 1992; Stark and Perkel 1999; Scott et al. 2004). Blocking the RA receptors of the AFP outflow prevents song modifications during training (Warren et al. 2011; Charlesworth et al. 2012). Injections of brain-derived neurotrophic factor (BDNF) into RA disrupt adult song stability by increasing the frequency of HVC axonal boutons in RA (Kittelberger and Mooney 2005). It is therefore reasonable to presume that the neural plasticity in RA is needed for deafening-induced learned vocal changes and such cortical plasticity is controlled by the basal ganglia circuit.

Here we demonstrate that deafening induces marked effects on synaptic structures in RA in adult zebra finches, including changes in dendritic spine density and morphology. Specifically, we find different morphological alterations of spine synaptic contacts between the LMAN–RA and HVC–RA pathways, in response to hearing loss. We further show that disruption of the basal ganglia circuit, via lesions to Area X, can prevent plastic changes to RA dendritic spines. Thus, our results provide direct cellular evidence that motor cortical plasticity is required for deafening-induced learned vocal changes, and that such plasticity is largely dependent on the function of the basal ganglia circuit. More generally, our findings provide important clues for understanding the neural mechanisms underlying speech control and plasticity in humans.

Materials and Methods

Animals

Young adult male zebra finches (4–6 months post-hatch, 48 animals) were purchased from a local breeder and housed individually in sound-attenuated chambers on a 12:12 h light/dark cycle with free access to food and water. All procedures were approved by the Animal Management Committee of the College of Life Sciences, Beijing Normal University.

Surgery

Birds were deafened by bilateral cochlear removal, following Li et al. (2013). The extracted cochlea was verified to be complete under a microscope. In a subset of these birds (i.e., lesion-deaf birds, $n = 7$), bilateral electrolytic lesions of Area X (50 μA for 30 s at each of 10–12 sites per hemisphere) were made 7 days before deafening, with the aid of a stereotaxic apparatus with a head angle of 30° relative to the horizontal plane to avoid damaging LMAN. Area X lesions were also made in another group of birds with intact hearing (i.e., lesion-hearing birds, $n = 4$). Electrolytic lesions were used, as opposed to neurotoxic lesions, to minimize Area X recovery from the surgery (Kubikova et al. 2014). But a limitation of electrolytic lesions is that it may possibly damage DLM axons in passage through the Area X to enter the LMAN (Boettiger and Doupe 1998; Kubikova et al. 2007). Lesions were evaluated histologically using Nissl staining (Cresyl violet acetate, C-5042, Sigma) and GluR1 immunostaining (Wada et al. 2004; AB1504, Millipore, diluted 1:800). Remaining Area X volumes were measured and compared with volumes from control birds with intact brains ($n = 3$). Lesion sizes of Area X ranged from 73 to 92%.

Song Analysis

Undirected song was recorded continuously with Sound Analysis Pro (version 2011.104; Tchernichovski et al. 2000). Changes in song structure after surgery were measured using the same software. The dominant motif for each bird was defined by visual inspection throughout the recordings before and after surgery. Thirty examples of the dominant motif were selected for analysis from each bird per time-point. We quantified 2 syllable spectral features, namely Wiener entropy and Wiener entropy variance. We examined their mean values as well as their variability across repeated renditions, presented as the coefficient of variation (CV = standard deviation/|mean|). The values from 2 preoperative days (0–2 days before deafening, for birds deafened only, or before lesioning, for lesion-deaf and lesion-hearing birds) were averaged to obtain the baseline level for each measure. The degree of change for those parameters on the last survival day was expressed as a percentage of the baseline.

Neuronal Tracing

Birds were anesthetized with sodium pentobarbital (60 mg/kg) and placed in a stereotaxic head holder at an angle of 45°. Neuronal anterograde tracers were injected into LMAN (Alexa-Fluor 488 conjugated dextran amine, 5% in PBS, D-22910, Molecular Probes; 165.6 nL per injection, total injection volume ~0.5 μL, 3 sites per hemisphere) and HVC (Alexa-Fluor 647 conjugated dextran amine, 5% in PBS, D-22914, Molecular Probes; 82.8 nL per injection, total injection volume ~0.5 μL, 6 sites per hemisphere) through a glass pipette attached to a Nanoject-II microinjector (Drummond Scientific). Birds survived for 7 days, to allow for the transportation of tracers to the RA. After sacrifice, DiI labeling of RA dendritic spines was performed as described below. Only birds with accumulated tracers distributed throughout RA were chosen for double-labeling analysis.

Fluorescent Labeling of Dendritic Spines

RA dendritic spines were labeled with the carbocyanine dye DiI (1,1′-dioctadecyl-3,3,3′,3′-tetramethylindocarbocyanine

perchlorate, D-282, Molecular Probes) according to the protocol described previously (Kim et al. 2007; Rasia-Filho et al. 2010). Briefly, birds were overdosed with urethane and perfused with 1.5% paraformaldehyde (PFA) in 0.1 M PB. The brains were sagittally sectioned into 150 µm slices with a vibratome and collected in PB. Sonicated fine powdered DiI was gently applied over the RA using a glass micropipette under a dissecting microscope. Slices were incubated in PB at room temperature for 12–14 h in the dark to allow the full diffusion of DiI along the neuronal membranes. After further fixation (4% PFA, 30 min), the slices were mounted under coverslip with anti-fading mounting media (H-1000, Vector Laboratories Inc.).

Confocal Microscopy

A Zeiss LSM 700 confocal microscope was used to image the labeled sections. Sections were inspected first at low magnification for localizing DiI-labeled spiny neurons within RA. DiI was excited using a HeNe 555-nm laser line (a "red" channel). The sampled RA spiny neurons were randomly distributed within the nucleus without site preference. For each neuron, 1–5 s- or third-order dendrite segments of 30–75 µm in length separated from the soma by about 50 µm were sampled. For double-labeling quantifications, Alexa Fluor 488- or 647-labeled axon terminals were scanned in the corresponding paired channel (a "green" channel with 488 nm excitation or an "infrared" channel with 639 nm excitation) together with DiI imaging using a high-resolution immersion objective (40×, numerical aperture 1.3, zoom 3, pinhole 1 arbitrary unit, averaging 2, 1024 × 1024 pixels, z-step 0.2 µm), with optimal settings for gain and offset. For single DiI imaging, image stacks were acquired at 512 × 512 pixel resolution with a z-step of 0.15 µm. Image stacks were then deconvolved using a blind deconvolution algorithm (AutoQuant, Media Cybernetics) before quantification.

Dendritic spines were analyzed by NeuronStudio software (Rodriguez et al. 2008). Spines were defined as dendritic protrusions with lengths between 0.5 and 3 µm, and visible head diameters (>0.1 µm). Spine length and spine head diameter (or spine width) were measured automatically. Spine density (number per 10 µm segment) was calculated by dividing the number of spines present by the length of the dendritic segment in micrometers, and multiplying by 10.

For synaptic contact analysis, image stacks were processed using ImageJ (NIH) and Zen (Zeiss). To identify 3-dimensional (3D) boutons in images obtained in the "green" or "infrared" channel, we used the mean gray intensity value plus 3 standard deviations as an objective threshold, which was determined using ImageJ 3D object-threshold analysis (plugin "3D object counter") for each stack. Based on the threshold for bouton recognition, synaptic contacts between tracer-labeled boutons and DiI-labeled dendrites were identified and counted manually via ImageJ and Zen, according to the following criteria: (1) a distance between channels of no more than one pixel at the site of the presumed contact, (2) the existence of overlap in at least 2 optical planes in a orthogonal section, and (3) the existence of overlap in at least 2 sections along the z-axis. The spine contact ratio was then calculated by dividing the number of contacts with spines by the total number of contacts present for each dendritic segment.

Electron Microscopy

Birds were anesthetized with a lethal dose of urethane and perfused transcardially with 0.9% NaCl, followed by a solution containing 4% paraformaldehyde and 0.5% glutaraldehyde in 0.1 M PB. The brains were sliced into 100 µm sagittal sections with a vibrating microtome. Tissue pieces of RA were dissected out using a punch needle with a 0.7 mm inside diameter. These pieces were post-fixed in 1% osmium tetroxide, dehydrated in a graded series of ethanol, and flat embedded in Epon 812 (Electron Microscopy Sciences). Following semithin sectioning, ultrathin sections (50–70 nm) were cut with a LEICA ultramicrotome, mounted on 200-mesh grids, counterstained with lead citrate and uranyl acetate, and finally viewed and photographed with an FEI Tecnai G2 Spirit electron microscope at an accelerating voltage of 120 kV. For each bird, at least 50 micrographs (20 500×, 12.3 μm^2) were randomly captured throughout the neuropil within RA for quantification. Asymmetric synapses were identified by the presence of a postsynaptic membrane density (PSD) and presynaptic clear vesicles adjacent to the PSD. Synapses located on dendritic spines or shafts were confirmed on sequential sections. The density of asymmetric synapses (number of synapses per 100 μm^2) was measured with the aid of ImageJ.

Statistics

All statistical analyses were performed using SPSS 13.0 (SPSS, Chicago, IL) and GraphPad Prism 5.0 for Windows (GraphPad Software, San Diego, CA). Normality was tested using the one-sample Kolmogorov–Smirnov (KS) test. Comparisons of mean values in spine density and morphology data (length and width) were performed using unpaired *t*-tests (between control and deaf birds), or one-way ANOVA followed by Tukey's post hoc test (among 4 groups: control, deaf, lesion-deaf, and lesion-hearing). The 2-sample KS test was used to compare cumulative frequency distributions for spine morphology between the groups. For non-normally distributed data, such as differences in the HVC/LMAN-RA spine contact ratio between control and deaf birds, and the degree of change in syllable features among the 4 groups, the nonparametric Mann–Whitney *U* test and Kruskal–Wallis test (followed by Dunn's post hoc test) were applied. In all analyses, 2-tailed *P*-values <0.05 were considered to be statistically significant. Graphs were prepared with GraphPad Prism 5.0. All data were expressed as mean ± standard error of the mean (SEM).

Results

Deafening Causes Structural Changes to Dendritic Spines in Adult RA

Zebra finch RA contains 2 morphological types of neurons, spiny, and aspious (Spiro et al. 1999). Here, we focused on spiny neurons, which are putative projection neurons (Spiro et al. 1999). The majority of RA projection neurons are known to be pivotal in learned vocal control by providing cortical motor output to brainstem nuclei controlling syringeal and respiratory muscles for singing (Vicario 1991; Wild 1997). RA also contains small neuron populations projecting to the DLM (Wild 1993) and to the HVC (Roberts et al. 2008), thus forming circuits that are similar to cortico-thalamic connectivity and reciprocal cortical connections of mammalian primary motor cortex, respectively (Jones et al. 1978; Kultas-Ilinsky et al. 2003). Using the fluorescent dye DiI on brain slices, RA spiny neurons as well as their dendrites and dendritic spines were well labeled (Fig. 1A and Supplementary Fig. 1). These DiI-labeled neurons could have different targets as described above, though we did not identify them in the present study. For each neuron, second- and third-order dendrites were

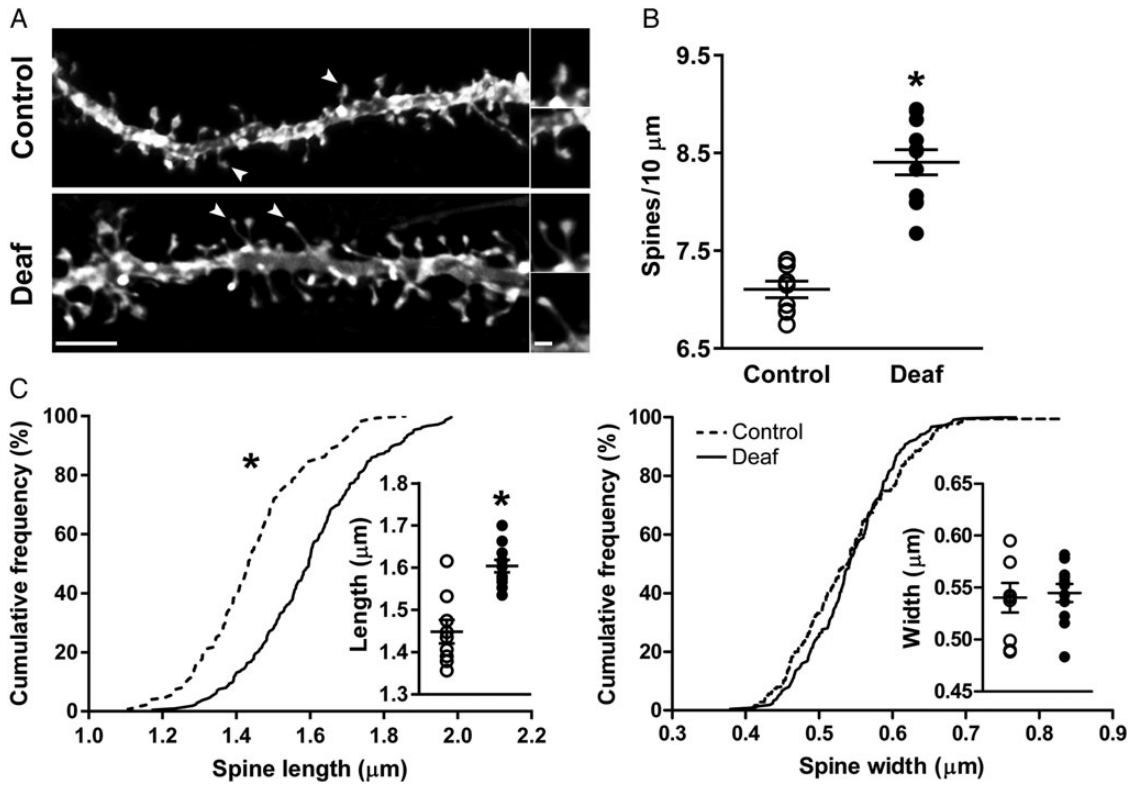

Figure 1. Deafening causes increases in spine density and spine length in adult RA. (*A*) Representative images of DiI-labeled dendrites of RA spiny neurons from a control and a deafened bird. Arrowheads indicate dendritic spines. Scale bars are 5 μm in the left panel and 1 μm in the right panel. (*B*) Quantification of dendritic spine density in control ($n = 9$ birds, 175 dendrites from 76 cells in birds with intact cochleae) and deaf conditions ($n = 11$ birds, 214 dendrites from 99 cells in birds deafened by bilateral cochlear removal). A total of 6796 and 9765 spines were measured in control and deafened birds, respectively, from images acquired at 1024 × 1024 pixel resolution. Data are presented as scattergrams (with mean ± SEM superimposed, one point per bird). *$P < 0.0001$, unpaired *t*-test. (*C*) Cumulative frequency plots of spine length (left, *$P < 0.0001$, KS test) and spine head diameter (right, $P = 0.1$, KS test) from the same set of data (control, $n = 175$ dendrites; deaf, $n = 214$ dendrites). Inset scattergrams show values of individual control and deafened birds (with mean ± SEM superimposed; left, *$P < 0.0001$; right, $P = 0.78$; unpaired *t*-test).

imaged and measured. We evaluated the effect of deafness on their dendritic spine structure, including spine density and spine morphology. We found that the mean spine density was significantly increased, by about 18%, in deafened birds by 14 days after deafening, when compared with control birds with intact cochleae (Fig. 1*A*,*B*; control, 7.1 ± 0.08 spines per 10 μm; deaf, 8.41 ± 0.13 spines per 10 μm; $P < 0.0001$, unpaired *t*-test). An increase in the spine length also occurred in deafened birds, compared with controls (Fig. 1*A*,*C*, left; control, 1.45 ± 0.03 μm; deaf, 1.6 ± 0.01 μm; $P < 0.0001$, KS test, unpaired *t*-test), whereas the spine width in deafened birds was still comparable to the controls over the same time course (Fig. 1*C*, right; control, 0.54 ± 0.01 μm; deaf, 0.54 ± 0.009 μm; $P = 0.1$, KS test; $P = 0.78$, unpaired *t*-test). Because dendritic spines form the postsynaptic specialization of the vast majority of excitatory synapses (Kasai et al. 2010; Yu and Zuo 2011), deafening-induced structural changes to RA dendritic spines indicate a significant reorganization of their synaptic connections following deafening.

We confirmed the spine synaptic changes in RA using high-resolution electron microscopy (EM) at 14 days after hearing loss (Fig. 2*A*). The mean density of asymmetric synapses (shown to be excitatory synapses, Harris and Weinberg 2012) formed on dendritic spines was increased significantly, by about 38%, in deafened birds compared with control birds (Fig. 2*B*; control, 7.97 ± 0.18 synapses per 100 μm^2; deaf, 11.0 ± 0.3 synapses per 100 μm^2; $P < 0.0001$, unpaired *t*-test). Concomitantly, a significant increase in the mean density of asymmetric synapses formed on dendritic shafts occurred in deafened birds (Fig. 2*B*; control, 8.41 ± 0.53 synapses per 100 μm^2; deaf, 12.19 ± 0.23 synapses per 100 μm^2; $P = 0.0002$, unpaired *t*-test). The synaptic density values in RA for our control birds were consistent with a previous report (Herrmann and Arnold 1991). Taken together, we demonstrated that deafening caused rapid synaptic structural changes in adult RA.

Deafening Induces Structural Changes to RA Spine Synaptic Contacts From the LMAN and HVC

Individual RA spiny neurons receive afferent inputs that originate from the LMAN and the HVC (Mooney and Konishi 1991). To examine the possible contributions of these 2 pathways to adult vocal plasticity induced by deafening, we injected neural tracers with distinct colors into the LMAN and the HVC (Fig. 3*A* and Supplementary Fig. 2). In combination with DiI staining, we could observe the synaptic contacts on dendrites of RA spiny neurons from either the LMAN or the HVC. Consistent with a previous study (Herrmann and Arnold 1991), we confirmed that there were synaptic contacts from the LMAN or the HVC located on both the dendritic shafts and the spines (Fig. 3*B*). Furthermore, by 2 weeks after deafening, along with the increase in spine density, the proportion of synaptic contacts on dendritic spines as opposed to total contacts on dendrites was significantly increased from both the LMAN (control, 0.33 ± 0.02, $n = 100$ dendrites from 39 cells in 5 birds; deaf, 0.45 ± 0.02, $n = 126$ dendrites from 57 cells in 7 birds; $P < 0.0001$, Mann–Whitney *U* test) and the

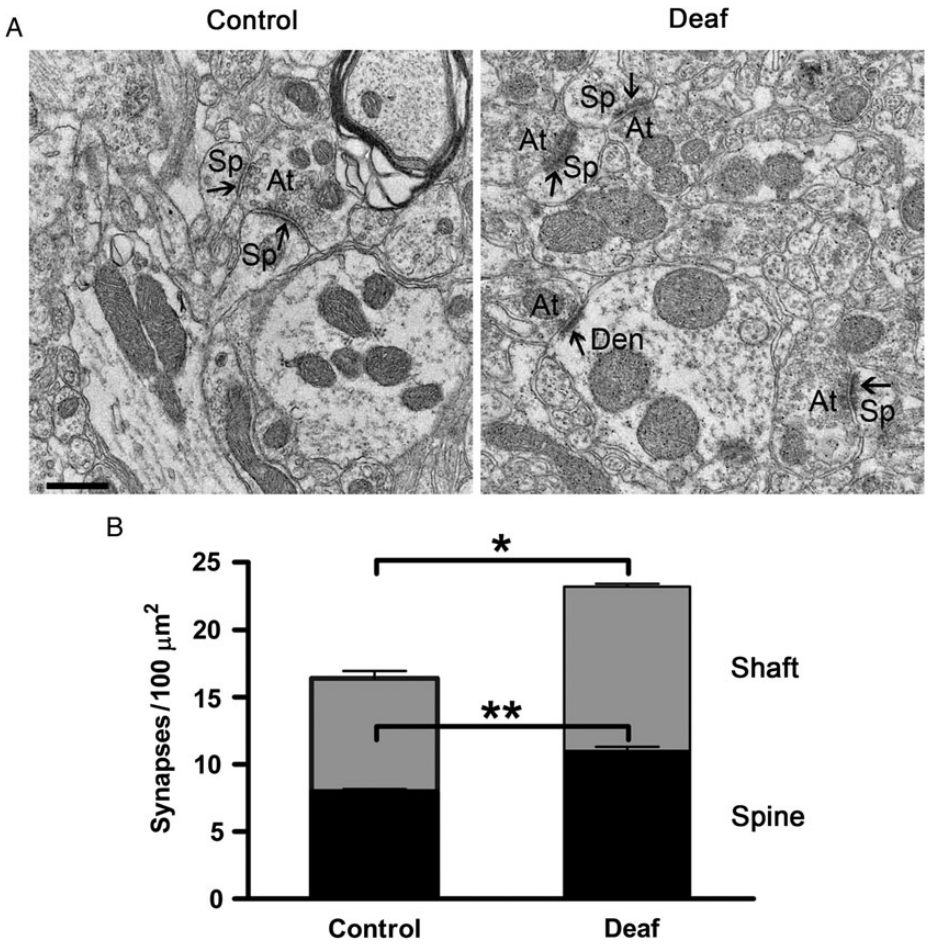

Figure 2. Effects of deafening on asymmetric synapses in adult RA. (*A*) Representative electron micrographs of RA in a control and a deafened bird show axon terminals (At) synapsing (arrows) with dendritic spines (Sp) or dendritic shafts (Den). Scale bar is 0.5 μm. (*B*) Comparison of synapse density (mean ± SEM; bottom, spine synapses; top, shaft synapses) between control ($n = 6$) and deafened birds ($n = 5$). *$P = 0.0002$, **$P < 0.0001$, unpaired *t*-test.

HVC (control, 0.45 ± 0.02, $n = 120$ dendrites from 51 cells in 6 birds; deaf, 0.55 ± 0.02, $n = 124$ dendrites from 55 cells in 6 birds; $P < 0.0001$, Mann–Whitney *U* test), indicating that deafening caused a significant rearrangement of synaptic contacts on RA spiny neurons in both pathways.

We further found that spine morphology was considerably different between the LMAN-RA and HVC–RA pathways under normal conditions. HVC-RA spines appeared much longer and wider than LMAN-RA spines (Fig. 3C, left; length: control-HVC, 1.68 ± 0.03 μm; control-LMAN, 1.52 ± 0.04 μm; $P = 0.003$, KS test; Fig. 3C, right; width: control-HVC, 0.64 ± 0.01 μm; control-LMAN, 0.54 ± 0.02 μm; $P < 0.0001$, KS test). In addition, spines in the 2 pathways responded differently to hearing loss. Deafening induced a marked elongation of LMAN-RA spines, but the length of HVC-RA spines was relatively stable (Fig. 3C, left; deaf-LMAN, 1.81 ± 0.03 μm; control-LMAN vs. deaf-LMAN, $P < 0.0001$, KS test; deaf-HVC, 1.77 ± 0.03 μm; control-HVC vs. deaf-HVC, $P = 0.06$, KS test). Spine width did not change measurably in either pathway (Fig. 3C, right; deaf-LMAN = 0.56 ± 0.01 μm, deaf-HVC = 0.62 ± 0.01 μm; control-LMAN vs. deaf-LMAN, $P = 0.57$, KS test; control-HVC vs. deaf-HVC, $P = 0.29$, KS test). Overall, we demonstrated that the spine morphology of RA neurons in the 2 pathways was quite distinct under the normal conditions, and that LMAN-RA spines appeared to be more sensitive in response to deafening.

Changes to RA Dendritic Spines and Song Behavior Induced by Deafening are Largely Prevented by Area X Electrolytic Lesions

The above findings suggest that the AFP may play an important role in deafening-induced RA spine plasticity, rather than HVC–RA pathway. To investigate a possible upstream source in the AFP that drives this cortical plasticity, we made electrolytic lesions of the AFP input nucleus Area X ahead of deafening (see Supplementary Fig. 3), because the basal ganglia nucleus Area X is recently shown to be required for learned song plasticity (Ali et al. 2013; Kojima et al. 2013). While considering a limitation of the electrolytic lesion technique (see Material and Methods for details), we could not rule out damage to DLM fibers of passage in addition to Area X destruction. We found that the deafening-induced increase in RA spine density was blocked by the lesions, whereas this disruption did not affect spine density in hearing birds, compared with controls, in the same time frame (Fig. 4A,B; control, 6.78 ± 0.11 spines per 10 μm; deaf, 8.37 ± 0.09 spines per 10 μm; lesion-deaf, 6.68 ± 0.13 spines per 10 μm; lesion-hearing, 6.99 ± 0.04 spines per 10 μm; control vs. deaf, $P < 0.0001$; control vs. lesion-deaf, $P = 0.9$; control vs. lesion-hearing, $P = 0.66$; one-way ANOVA followed by Tukey's post hoc test). This indicates a dominant role for the Area X (possibly and/or the DLM) in regulating plasticity of RA spine density. The deafening-induced

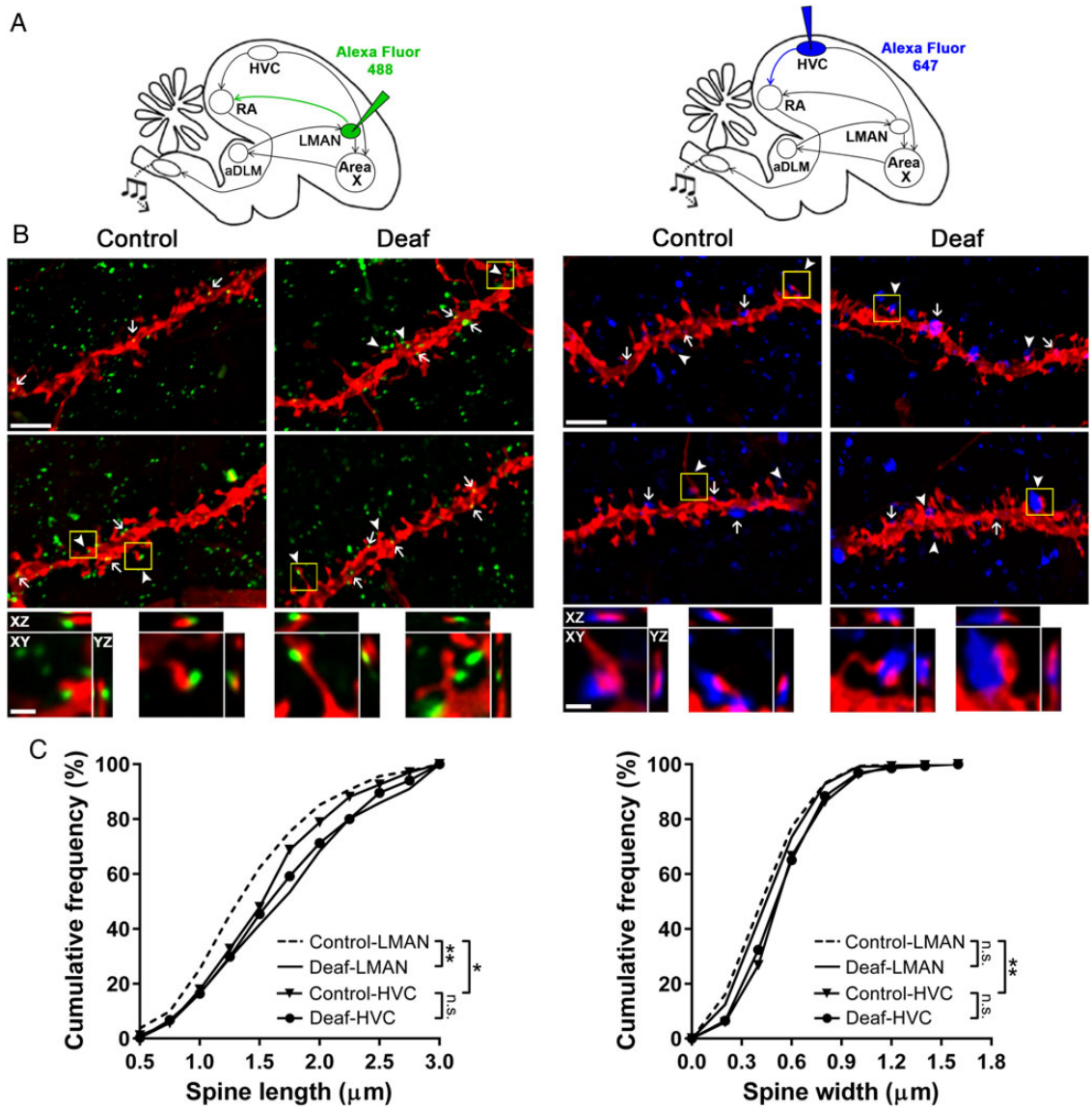

Figure 3. Morphological differences between dendritic spines in the LMAN–RA and HVC–RA pathways both under normal conditions and in response to hearing loss. (*A*) Schematic depiction of the song circuit, showing the injection of Alexa Fluor 488 and 647 dextrans in the LMAN (left) and the HVC (right), respectively. The fluorescent tracer can be anterogradely transported along the LMAN or HVC axons into RA. The aDLM is the anterior portion of the dorsal lateral nucleus of the medial thalamus. (*B*) Representative composite images taken from confocal image stacks, illustrating contacts between postsynaptic dendrites (DiI, red) of RA spiny neurons and presynaptic LMAN boutons (green, left) or HVC boutons (blue, right), from control and deafened birds. Arrowheads and arrows indicate bouton-spine and bouton-shaft pairs, respectively. Scale bar is 5 μm. The spine synaptic contact outlined with a box is shown enlarged in the bottom panel, in which the overlap between the spine and the bouton in the z-axis can also be seen. Scale bar is 1 μm. (*C*) Cumulative frequency plots of the morphology of spines in contact with LMAN boutons or HVC boutons in control and deafened birds (left, length; right, width; control-LMAN, $n = 162$ spines, 84 dendrites from 39 cells in 5 intact birds; deaf-LMAN, $n = 347$ spines, 117 dendrites from 57 cells in 7 deafened birds; control-HVC, $n = 269$ spines, 111 dendrites from 51 cells in 6 intact birds; deaf-HVC, $n = 355$ spines, 118 dendrites from 55 cells in 6 deafened birds). *$P < 0.001$, **$P < 0.0001$, n.s., not significant, KS test.

increase in RA spine length was also eliminated by the presence of lesions before deafening. But considerable trend of spine elongation was observed in lesion-hearing birds, though the statistical significance obtained at the dendrite level disappeared at the bird level (Fig. 4C, top; control, 1.47 ± 0.03 μm; deaf, 1.59 ± 0.03 μm; lesion-deaf, 1.43 ± 0.03 μm; lesion-hearing, 1.55 ± 0.03 μm; control vs. deaf, KS test, $P < 0.0001$; one-way ANOVA, $P = 0.02$; control vs. lesion-deaf, KS test, $P = 0.66$; one-way ANOVA, $P = 0.74$; control vs. lesion-hearing, KS test, $P < 0.0001$; one-way ANOVA, $P = 0.37$). The contrasting effects of the lesions on RA spine length in hearing and deaf situations indicate a dual role of the Area X (possibly and/or the DLM) in regulating RA spine length. This finding also suggests that, besides the Area X (possibly and/or the DLM), both maintenance of RA spine length in normal adults and changes after deafening might rely on additional components of the song system. We also found an obvious decline in the spine width in the lesion-deaf group—although statistical significance at the dendrite level disappeared at the bird level—while it remained unchanged in both deafened and lesion-hearing birds, when compared with controls (Fig. 4C, bottom; control, 0.59 ± 0.01 μm; deaf, 0.59 ± 0.01 μm; lesion-deaf, 0.55 ± 0.006 μm; lesion-hearing, 0.58 ± 0.02 μm; control vs. deaf, KS test, $P = 0.92$; one-way ANOVA, $P = 0.99$; control vs. lesion-deaf, KS test, $P < 0.0001$; one-way ANOVA, $P = 0.14$; control vs.

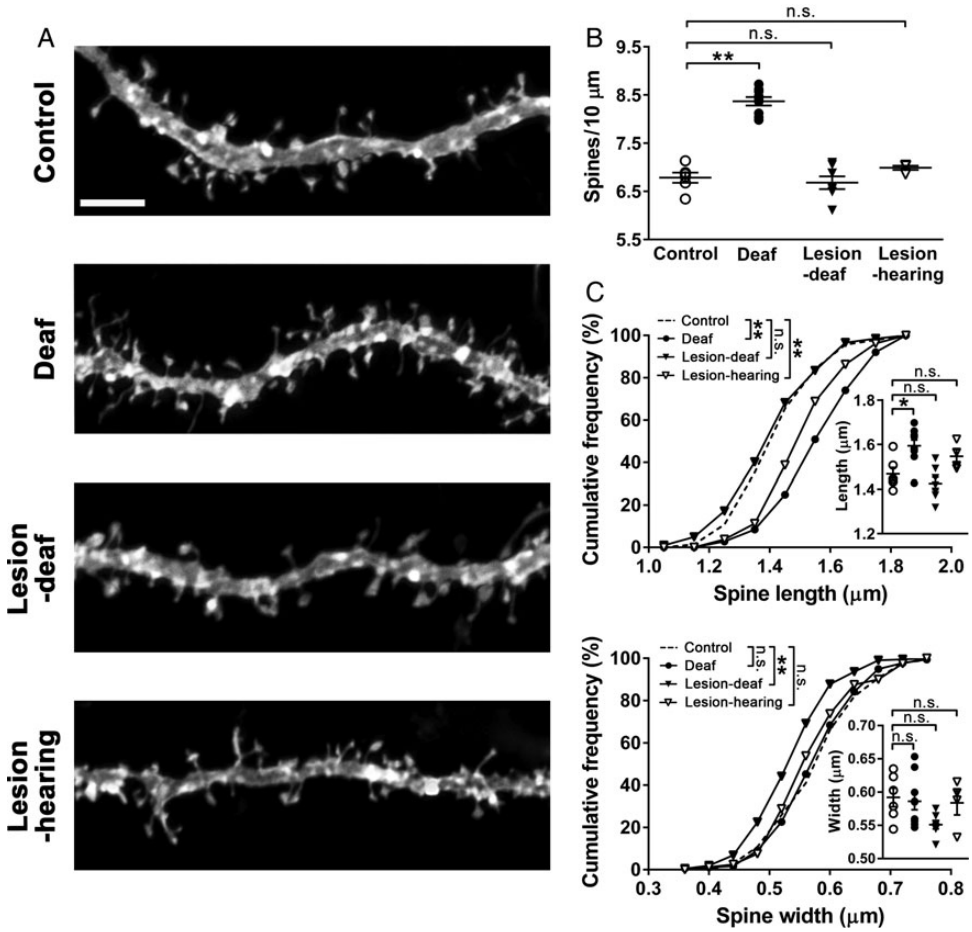

Figure 4. Area X electrolytic lesions eliminate deafening-induced changes in spine density and spine length in RA. (*A*) Representative images of DiI-labeled dendrites of RA spiny neurons from 4 groups. Scale bar is 5 µm. (*B*) Quantification of dendritic spine density in 4 groups (control, $n = 6$ birds, 5259 spines on 139 dendrites from 54 cells; deaf, $n = 9$ birds, 8144 spines on 177 dendrites from 70 cells; lesion-deaf, $n = 7$ birds, 7041 spines on 204 dendrites from 92 cells; lesion-hearing, $n = 4$ birds, 3726 spines on 80 dendrites from 27 cells; data from images acquired at 512 × 512 pixel resolution). Data are presented as scattergrams (with mean ± SEM superimposed, one point per bird). **$P < 0.0001$, one-way ANOVA followed by Tukey's post hoc test. (*C*) Cumulative frequency plots of spine length (top) and width (bottom) from the same set of data (control: $n = 139$ dendrites, deaf: $n = 177$ dendrites, lesion-deaf: $n = 184$ dendrites, lesion-hearing: $n = 80$ dendrites; **$P < 0.0001$, KS test). Inset scattergrams show values for individual birds in 4 groups (with mean ± SEM superimposed). *$P = 0.02$, one-way ANOVA followed by Tukey's post hoc test.

lesion-hearing, KS test, $P = 0.09$; one-way ANOVA, $P = 0.98$). We therefore speculate that maintenance of spine head morphology after deafening might result from a balance between the Area X (possibly and/or the DLM) and other components of the song system. Taken together, these findings demonstrated a key role of the Area X (possibly and/or the DLM) for deafening-induced plasticity of RA dendritic spine density and morphology, although changes in spine morphology could not be fully explained.

To evaluate the relationship between RA spine structural plasticity and vocal behavior, we examined birds' song structure using 2 syllable spectral features, Wiener entropy and entropy variance. These parameters have been reported to be the most sensitive to deafness, and to change during the first 2 weeks after deafening (Horita et al. 2008; Tschida and Mooney 2012). Here the degree of change in each measure for each syllable was calculated as the percentage of its baseline level, the average of 2 preoperative days (–2 to 0). We confirmed that a robust increase in mean entropy, as well as a pronounced decline in mean entropy variance, occurred in deafened birds by 14 days after deafening, in comparison with controls (Fig. 5*A*,*B*, top; entropy: control, 100.5 ± 0.62; deaf, 93.6 ± 0.96; control vs. deaf, $P < 0.0001$; entropy variance: control, 104.7 ± 4.13; deaf, 84.9 ± 3.09; control vs. deaf, $P = 0.003$; Kruskal–Wallis test followed by Dunn's post hoc test). We also found that the variation in these 2 features across song renditions considerably increased after deafening (Fig. 5*B*, bottom; entropy CV: control, 107.1 ± 3.79; deaf, 143.9 ± 8.25; control vs. deaf, $P = 0.02$; entropy variance CV: control, 99.7 ± 3.83; deaf, 125.2 ± 5.78; control vs. deaf, $P = 0.008$; Kruskal–Wallis test followed by Dunn's post hoc test). However, Area X electrolytic lesions appeared to largely prevent such deafening-induced behavioral changes (Fig. 5*A*,*B*; entropy: 96.1 ± 1.54; control vs. lesion-deaf, $P = 0.05$; entropy variance: 103.4 ± 6.37; control vs. lesion-deaf, $P = 1.0$; entropy CV: 128.1 ± 7.35; control vs. lesion-deaf, $P = 0.42$; entropy variance CV: 100.4 ± 5.87; control vs. lesion-deaf, $P = 1.0$; Kruskal–Wallis test followed by Dunn's post hoc test), whereas lesions in hearing birds did not markedly affect their normal song structure (Fig. 5*A*,*B*; entropy: 101.1 ± 1.25; control vs. lesion-hearing, $P = 1.0$; entropy variance: 90.1 ± 5.11; control vs. lesion- hearing, $P = 0.42$; entropy CV: 125.3 ± 6.84; control vs. lesion-hearing, $P = 0.66$; entropy variance CV: 117.7 ± 9.83; control vs. lesion-hearing, $P = 0.72$; Kruskal–Wallis test followed by Dunn's post hoc test). These findings are consistent with a previous report that deafening-induced adult song plasticity can be prevented by neurotoxic lesions of Area X (Kojima et al. 2013),

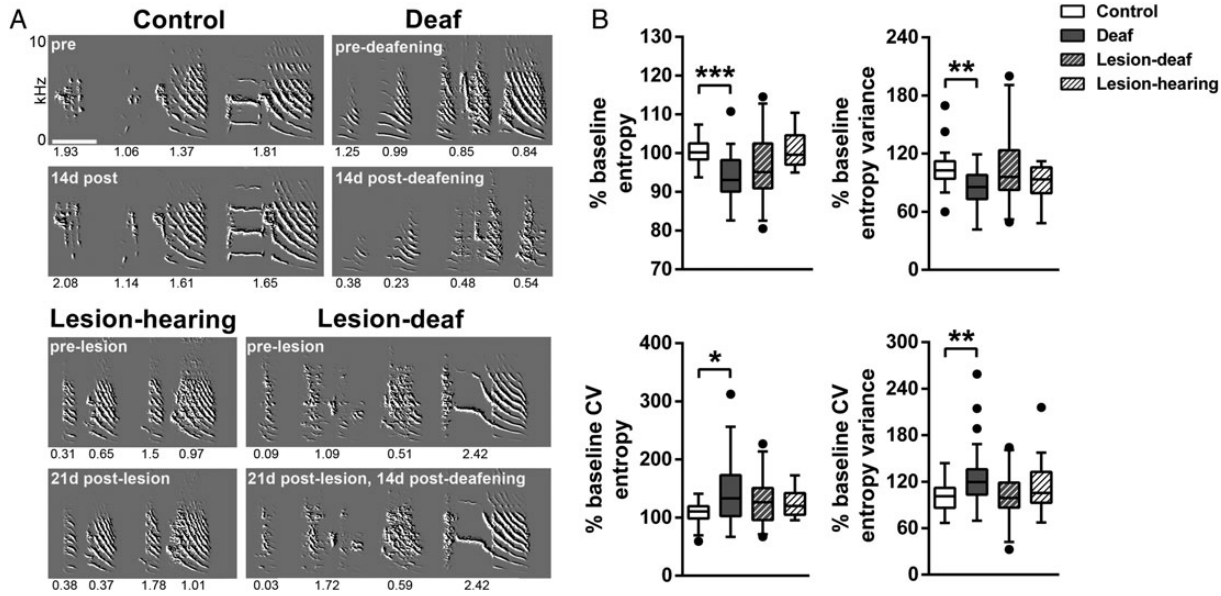

Figure 5. Deafening-induced song deterioration can be prevented by Area X electrolytic lesions. (*A*) Representative spectrograms show pronounced changes in syllable structures in a deafened bird (top right), whereas relatively stable structures are maintained in a control bird with intact cochleae (top left), a bird with lesions at 7 days before deafening (bottom right) and a hearing bird with lesions (bottom left). Pre- and postoperative songs are presented and the value of the mean entropy variance is shown below each syllable. Frequency range (*y* axis), 0–10 kHz. Scale bar is 100 ms. (*B*) Quantification of changes in syllable spectral features (mean entropy and entropy variance) and their variability across repeated renditions (coefficient of variation, CV) at postoperative day 14 (in control and deafened birds) or day 21 (in lesion-deaf and lesion-hearing birds). The degree of change in each measure for each syllable was expressed as a percentage of its baseline level, which was obtained from 2 preoperative days. Box-and-whisker plots show the distributions of changes to syllables for each of the 4 groups (control, $n = 25$ syllables in 6 birds; deaf, $n = 40$ syllables in 9 birds; lesion-deaf, $n = 29$ syllables in 7 birds; lesion-hearing, $n = 14$ syllables in 4 birds). The box denotes the interquartile range, whiskers denote 1.5 interquartile ranges, and the horizontal line within each box denotes the median. $^{*}P < 0.05$, $^{**}P < 0.01$, $^{***}P < 0.0001$, Kruskal–Wallis test followed by Dunn's post hoc test.

which is considered to minimize damage to passage fibers (Kubikova et al. 2007). Taken together, these findings suggest that deafening-induced learned vocal alteration occur in parallel with RA spine structural changes.

Discussion

By visualizing dendritic spine structural changes in zebra finches, our study demonstrates rapid deafening-induced synaptic plasticity in the adult vocal motor cortex RA, accompanied with song degradation. We have uncovered morphological differences in RA spines between 2 major afferent pathways, and further highlighted a key role of the basal ganglia circuit in the motor cortical plasticity.

Dendritic spines are known to be the major sites of excitatory synaptic transmission, and their morphology and density influence the functioning of neuronal circuits (Ultanir et al. 2007; Kasai et al. 2010; Yu and Zuo 2011). We suggest that structural changes to dendritic spines and spine synapses in the vocal motor cortex RA serve as an important cellular basis underlying deafening-induced vocal plasticity. These changes might disrupt signal processing within RA projection neurons, and consequently result in impairment of precise song control. Interestingly, these structural changes in the young adult RA appear to mirror the pattern in the RA during the normal developmental process of song learning, which is characterized by the elimination of the excess spine synapses that are initially produced (Herrmann and Arnold 1991). Our results therefore support the idea that adult vocal plasticity might use the same mechanisms as early vocal learning (Nordeen and Nordeen 2010).

Our study further demonstrates a considerable difference in spine morphology between 2 major pathways in RA, the LMAN–RA, and HVC–RA pathways, both under normal conditions and in response to hearing loss. HVC-RA spines are larger, suggesting a strong synaptic strength and supporting the dominant role of the HVC–RA pathway in driving adult stereotyped song (Herrmann and Arnold 1991; Yu and Margoliash 1996; Hahnloser et al. 2002; Aronov et al. 2008; Garst-Orozco et al. 2014). Consistently with this, HVC–RA spine morphology showed less sensitivity or a slower response to hearing loss, with only a minor change in length by 14 days after deafening. Conversely, the smaller spines in the LMAN–RA pathway might indicate their instability, supporting the role of the AFP in promoting vocal plasticity and variability (Williams and Mehta 1999; Brainard and Doupe 2001; Thompson et al. 2007). Indeed, LMAN–RA spines showed a rapid change in length within 2 weeks of deafening. We therefore speculate that deafening-induced synaptic changes in the LMAN–RA circuit might occur earlier than that in HVC–RA connections. This might explain recent behavioral data suggesting that the LMAN–RA circuit is involved in the initial vocal changes after deafening, or during reinforcement learning, whereas the VMP is required for enduring alterations in vocal behavior (Andalman and Fee 2009; Nordeen and Nordeen 2010). Aside from the morphological changes, both LMAN–RA and HVC–RA contacts shifted significantly from dendritic shafts to spines, along with an increase in spine density, by 2 weeks after deafening. Such remodeling likely disrupted the normal balance between the LMAN–RA and HVC–RA pathways in adult birds. The relative influence of VMP and AFP activity in RA seems to be critical for both song learning (Herrmann and Arnold 1991; Garst-Orozco et al. 2014) and maintenance (Thompson et al. 2007). But the exact deafening-induced changes in the relative strength of these 2 circuits need to be clarified in a future study.

Finally, we have shown that disruption of the basal ganglia circuit blocked deafening-induced spine structural changes in RA, suggesting that the activity of the basal ganglia circuit is

required for vocal plasticity, through its influence on motor cortical plasticity. Basal ganglia dysfunction is thought to affect plasticity of human motor cortex in Parkinson disease (Udupa and Chen 2013; Kishore et al. 2014). But how does the basal ganglia output influence plasticity of the vocal motor cortex? Kojima et al. (2013) recently reported that Area X lesions strip the singing-related bursting pattern of LMAN neurons, which appears to be critical for hearing-dependent vocal plasticity. This neuronal firing pattern might be important for regulating synaptic activity, including the secretion of neurotrophins such as BDNF (Edelmann et al. 2014), which is well known for its role in structural and functional synaptic plasticity in the vertebrate central nervous system (Deinhardt and Chao 2014). LMAN has been indicated to be an important source of BDNF in RA (Johnson et al. 1997), thereby contributing to RA synaptic plasticity. For example, in juvenile zebra finches, LMAN lesions result in a decrease in spine density for RA projection neurons, with a loss of song plasticity (Kittelberger and Mooney 1999). LMAN lesions also prevent deafening-induced, plasticity-related protein kinase C changes within adult RA (Watanabe et al. 2006). Therefore, deafening might change the levels of BDNF in RA by influencing the activity of the AFP. In this context, another important issue is the location where the auditory-related signals gain access to the song system to drive vocal plasticity. Sensorimotor nucleus HVC seems to be a promising candidate. Tschida and Mooney (2012) report that deafening induced rapid changes to dendritic spines of specific HVC neurons that project to Area X. But interestingly, by lesions of the AFP output nucleus LMAN, Hamaguchi et al. (2014) find that such changes in HVC rely on the AFP, thus indicating that the AFP accesses feedback independent of HVC. Here, by lesions of the AFP input part, our results further suggest that the auditory feedback-related signals enter the song system most likely via Area X to drive vocal plasticity. The large dopaminergic projection to Area X from the midbrain may convey this information from auditory cortical areas by a recently identified projection (Gale et al. 2008; Mandelblat-Cerf et al. 2014). In conclusion, we uncover deafening-induced plasticity in vocal motor cortex and demonstrate such cortical plasticity is driven by the basal ganglia circuit. These results provide a reasonable explanation for learned song plasticity. More generally, it could also be helpful to understand speech control and plasticity in humans.

Supplementary Material

Supplementary Material can be found at http://www.cercor.oxfordjournals.org/online.

Funding

This work was supported by the National Natural Science Foundation of China (grants: 30970360 and 31472001 to Y.Y.S., 31272310 to M.X.Z, and 31360517 to X.W.Z.).

Notes

We thank Z.X. Wang, S. Rosqvist, and B. Jack for their constructive comments on the manuscript. *Conflict of Interest*: None declared.

References

Albin RL, Young AB, Penney JB. 1989. The functional anatomy of basal ganglia disorders. Trends Neurosci. 12:366–375.

Ali F, Otchy TM, Pehlevan C, Fantana AL, Burak Y, Ölveczky BP. 2013. The basal ganglia is necessary for learning spectral, but not temporal, features of birdsong. Neuron. 80:494–506.

Andalman AS, Fee MS. 2009. A basal ganglia-forebrain circuit in the songbird biases motor output to avoid vocal errors. Proc Natl Acad Sci USA. 106:12518–12523.

Aronov D, Andalman AS, Fee MS. 2008. A specialized forebrain circuit for vocal babbling in the juvenile songbird. Science. 320:630–634.

Ashby FG, Turner BO, Horvitz JC. 2010. Cortical and basal ganglia contributions to habit learning and automaticity. Trends Cogn Sci. 14:208–215.

Bashir S, Mizrahi I, Weaver K, Fregni F, Pascual-Leone A. 2010. Assessment and modulation of neuroplasticity in rehabilitation with transcranial magnetic stimulation. PM R. 2:S253–S268.

Boettiger CA, Doupe AJ. 1998. Intrinsic and thalamic excitatory inputs onto songbird LMAN neurons differ in their pharmacological and temporal. J Neurophysiol. 79:2615–2628.

Bottjer SW, Miesner EA, Arnold AP. 1984. Forebrain lesions disrupt development but not maintenance of song in passerine birds. Science. 224:901–903.

Brainard MS, Doupe AJ. 2000. Interruption of a basal ganglia-forebrain circuit prevents plasticity of learned vocalizations. Nature. 404:762–766.

Brainard MS, Doupe AJ. 2001. Postlearning consolidation of birdsong: stabilizing effects of age and anterior forebrain lesions. J Neurosci. 21:2501–2517.

Brainard MS, Doupe AJ. 2013. Translating birdsong: songbirds as a model for basic and applied medical research. Annu Rev Neurosci. 36:489–517.

Charlesworth JD, Warren TL, Brainard MS. 2012. Covert skill learning in a cortical-basal ganglia circuit. Nature. 486:251–255.

Cowie R, Douglas-Cowie E. 1992. Postlingually acquired deafness: speech deterioration and the wider consequences. Berlin: Mouton de Gruyter.

Deinhardt K, Chao MV. 2014. Shaping neurons: Long and short range effects of mature and proBDNF signalling upon neuronal structure. Neuropharmacology. 76(Pt C):603–609.

Doupe AJ, Perkel DJ, Reiner A, Stern EA. 2005. Birdbrains could teach basal ganglia research a new song. Trends Neurosci. 28:353–363.

Edelmann E, Lessmann V, Brigadski T. 2014. Pre- and postsynaptic twists in BDNF secretion and action in synaptic plasticity. Neuropharmacology. 76(Pt C):610–627.

Gale SD, Person AL, Perkel DJ. 2008. A novel basal ganglia pathway forms a loop linking a vocal learning circuit with its dopaminergic input. J Comp Neurol. 508:824–839.

Garst-Orozco J, Babadi B, Olveczky BP. 2014. A neural circuit mechanism for regulating vocal variability during song learning in zebra finches. eLife. 3:e03697.

Graybiel AM, Aosaki T, Flaherty AW, Kimura M. 1994. The basal ganglia and adaptive motor control. Science. 265:1826–1831.

Hahnloser RH, Kozhevnikov AA, Fee MS. 2002. An ultra-sparse code underlies the generation of neural sequences in a songbird. Nature. 419:65–70.

Hamaguchi K, Tschida KA, Yoon I, Donald BR, Mooney R. 2014. Auditory synapses to song premotor neurons are gated off during vocalization in zebra finches. eLife. 3:e01833.

Harris KM, Weinberg RJ. 2012. Ultrastructure of synapses in the mammalian brain. Cold Spring Harb Perspect Biol. 4:a005587.

Herrmann K, Arnold AP. 1991. The development of afferent projections to the robust archistriatal nucleus in male zebra finches: a quantitative electron microscopic study. J Neurosci. 11:2063–2074.

Horita H, Kobayashi M, Liu WC, Oka K, Jarvis ED, Wada K. 2012. Specialized motor-driven dusp1 expression in the song systems of multiple lineages of vocal learning birds. PLoS ONE. 7:e42173.

Horita H, Wada K, Jarvis ED. 2008. Early onset of deafening-induced song deterioration and differential requirements of the pallial-basal ganglia vocal pathway. Eur J Neurosci. 28:2519–2532.

Jarvis ED. 2004. Learned birdsong and the neurobiology of human language. Ann N Y Acad Sci. 1016:749–777.

Johnson F, Hohmann SE, DiStefano PS, Bottjer SW. 1997. Neurotrophins suppress apoptosis induced by deafferentation of an avian motor-cortical region. J Neurosci. 17:2101–2111.

Jones EG, Coulter JD, Hendry SH. 1978. Intracortical connectivity of architectonic fields in the somatic sensory, motor and parietal cortex of monkeys. J Comp Neurol. 181:291–347.

Kao MH, Doupe AJ, Brainard MS. 2005. Contributions of an avian basal ganglia-forebrain circuit to real-time modulation of song. Nature. 433:638–643.

Kasai H, Fukuda M, Watanabe S, Hayashi-Takagi A, Noguchi J. 2010. Structural dynamics of dendritic spines in memory and cognition. Trends Neurosci. 33:121–129.

Kim BG, Dai H-N, McAtee M, Vicini S, Bregman BS. 2007. Labeling of dendritic spines with the carbocyanine dye DiI for confocal microscopic imaging in lightly fixed cortical slices. J Neurosci Methods. 162:237–243.

Kishore A, Meunier S, Popa T. 2014. Cerebellar influence on motor cortex plasticity: behavioral implications for Parkinson's disease. Front Neurol. 5:68.

Kittelberger JM, Mooney R. 2005. Acute injections of brain-derived neurotrophic factor in a vocal premotor nucleus reversibly disrupt adult birdsong stability and trigger syllable deletion. J Neurobiol. 62:406–424.

Kittelberger JM, Mooney R. 1999. Lesions of an avian forebrain nucleus that disrupt song development alter synaptic connectivity and transmission in the vocal premotor pathway. J Neurosci. 19:9385–9398.

Kojima S, Kao MH, Doupe AJ. 2013. Task-related "cortical" bursting depends critically on basal ganglia input and is linked to vocal plasticity. Proc Natl Acad Sci USA. 110:4756–4761.

Kubikova L, Bosikova E, Cvikova M, Lukacova K, Scharff C, Jarvis ED. 2014. Basal ganglia function, stuttering, sequencing, and repair in adult songbirds. Sci Rep. 4:6590.

Kubikova L, Turner EA, Jarvis ED. 2007. The pallial basal ganglia pathway modulates the behaviorally driven gene expression of the motor pathway. Eur J Neurosci. 25:2145–2160.

Kultas-Ilinsky K, Sivan-Loukianova E, Ilinsky IA. 2003. Re-evaluation of the primary motor cortex connections with the thalamus in primates. J Comp Neurol. 457:133–158.

Lane H, Webster JW. 1991. Speech deterioration in postlingually deafened adults. J Acoust Soc Am. 89:859–866.

Lazard DS, Innes-Brown H, Barone P. 2014. Adaptation of the communicative brain to post-lingual deafness. Evidence from functional imaging. Hear Res. 307:136–143.

Leonardo A, Konishi M. 1999. Decrystallization of adult birdsong by perturbation of auditory feedback. Nature. 399: 466–470.

Li J, Zhou X, Huang L, Fu X, Liu J, Zhang X, Sun Y, Zuo M. 2013. Alteration of CaBP expression pattern in the nucleus magnocellularis following unilateral cochlear ablation in adult zebra finches. PLoS ONE. 8:e79297.

Lombardino AJ, Nottebohm F. 2000. Age at deafening affects the stability of learned song in adult male zebra finches. J Neurosci. 20:5054–5064.

Mandelblat-Cerf Y, Las L, Denisenko N, Fee MS. 2014. A role for descending auditory cortical projections in songbird vocal learning. eLife. 3:e02152.

Mooney R. 1992. Synaptic basis for developmental plasticity in a birdsong nucleus. J Neurosci. 12:2464–2477.

Mooney R, Konishi M. 1991. Two distinct inputs to an avian song nucleus activate different glutamate receptor subtypes on individual neurons. Proc Natl Acad Sci USA. 88:4075–4079.

Nordeen KW, Nordeen EJ. 1992. Auditory feedback is necessary for the maintenance of stereotyped song in adult zebra finches. Behav Neural Biol. 57:58–66.

Nordeen KW, Nordeen EJ. 2010. Deafening-induced vocal deterioration in adult songbirds is reversed by disrupting a basal ganglia-forebrain circuit. J Neurosci. 30:7392–7400.

Nottebohm F, Stokes TM, Leonard CM. 1976. Central control of song in the canary, *Serinus canarius*. J Comp Neurol. 165: 457–486.

Okanoya K, Yamaguchi A. 1997. Adult bengalese finches (*Lonchura striata* var. domestica) require real-time auditory feedback to produce normal song syntax. J Neurobiol. 33:343–356.

Pasley BN, Knight RT. 2013. Decoding speech for understanding and treating aphasia. Prog Brain Res. 207:435–456.

Pfenning AR, Hara E, Whitney O, Rivas MV, Wang R, Roulhac PL, Howard JT, Wirthlin M, Lovell PV, Ganapathy G, et al. 2014. Convergent transcriptional specializations in the brains of humans and song-learning birds. Science. 346:1256846.

Rasia-Filho A, Brusco J, Rocha L, Moreira J. 2010. Dendritic spines observed by extracellular DiI dye and immunolabeling under confocal microscopy. Protoc Exchange.

Roberts TF, Klein ME, Kubke MF, Wild JM, Mooney R. 2008. Telencephalic Neurons Monosynaptically Link Brainstem and Forebrain Premotor Networks Necessary for Song. J Neurosci. 28:3479–3489.

Rodriguez A, Ehlenberger DB, Dickstein DL, Hof PR, Wearne SL. 2008. Automated three-dimensional detection and shape classification of dendritic spines from fluorescence microscopy images. PLoS ONE. 3:e1997.

Scott LL, Singh TD, Nordeen EJ, Nordeen KW. 2004. Developmental patterns of NMDAR expression within the song system do not recur during adult vocal plasticity in zebra finches. J Neurobiol. 58:442–454.

Simonyan K. 2014. The laryngeal motor cortex: its organization and connectivity. Curr Opin Neurobiol. 28:15–21.

Simonyan K, Horwitz B, Jarvis ED. 2012. Dopamine regulation of human speech and bird song: A critical review. Brain Lang. 122:142–150.

Spiro JE, Dalva MB, Mooney R. 1999. Long-range inhibition within the zebra finch song nucleus RA can coordinate the firing of multiple projection neurons. J Neurophysiol. 81: 3007–3020.

Stark LL, Perkel DJ. 1999. Two-stage, input-specific synaptic maturation in a nucleus essential for vocal production in the zebra finch. J Neurosci. 19:9107–9116.

Tchernichovski O, Nottebohm F, Ho CE, Pesaran B, Mitra PP. 2000. A procedure for an automated measurement of song similarity. Anim Behav. 59:1167–1176.

Thompson JA, Wu W, Bertram R, Johnson F. 2007. Auditory-dependent vocal recovery in adult male zebra finches is facilitated by lesion of a forebrain pathway that includes the basal ganglia. J Neurosci. 27:12308–12320.

Tschida KA, Mooney R. 2012. Deafening drives cell type-specific changes to dendritic spines in a sensorimotor nucleus important to learned vocalizations. Neuron. 73: 1028–1039.

Udupa K, Chen R. 2013. Motor cortical plasticity in Parkinson's disease. Front Neurol. 4:128.
Ultanir SK, Kim J-E, Hall BJ, Deerinck T, Ellisman M, Ghosh A. 2007. Regulation of spine morphology and spine density by NMDA receptor signaling in vivo. Proc Natl Acad Sci USA. 104:19553–19558.
Vicario DS. 1991. Organization of the zebra finch song control system: II. Functional organization of outputs from nucleus robustus archistriatalis. J Comp Neurol. 309:486–494.
Wada K, Sakaguchi H, Jarvis ED, Hagiwara M. 2004. Differential expression of glutamate receptors in avian neural pathways for learned vocalization. J Comp Neurol. 476:44–64.
Waldstein RS. 1990. Effects of postlingual deafness on speech production: implications for the role of auditory feedback. J Acoust Soc Am. 88:2099–2114.
Warren TL, Tumer EC, Charlesworth JD, Brainard MS. 2011. Mechanisms and time course of vocal learning and consolidation in the adult songbird. J Neurophysiol. 106:1806–1821.
Watanabe A, Li R, Kimura T, Sakaguchi H. 2006. Lesions of an avian forebrain nucleus prevent changes in protein kinase C levels associated with deafening-induced vocal plasticity in adult songbirds. Eur J Neurosci. 23:2447–2457.
Wild JM. 1993. Descending projections of the songbird nucleus robustus archistriatalis. J Comp Neurol. 338:225–241.
Wild JM. 1997. Neural pathways for the control of birdsong production. J Neurobiol. 33:653–670.
Williams H, Mehta N. 1999. Changes in adult zebra finch song require a forebrain nucleus that is not necessary for song production. J Neurobiol. 39:14–28.
Woolley S, Rubel EW. 1997. Bengalese finches *Lonchura striata* domestica depend upon auditory feedback for the maintenance of adult song. J Neurosci. 17:6380–6390.
Yu AC, Margoliash D. 1996. Temporal hierarchical control of singing in birds. Science. 273:1871–1875.
Yu X, Zuo Y. 2011. Spine plasticity in the motor cortex. Curr Opin Neurobiol. 21:169–174.